Lesion Detection and Interobserver Agreement with Advanced Image Reconstruction for ^{18}F-DCFPyL PET/CT in Patients with Biochemically Recurrent Prostate Cancer

Bernard H.E. Jansen[1,2], Robin W. Jansen[1], Maurits Wondergem[3], Sandra Srbljin[4], John M.H. de Klerk[5], Birgit I. Lissenberg-Witte[6], André N. Vis[2], Reindert J.A. van Moorselaar[2], Ronald Boellaard[1], Otto S. Hoekstra[1], and Daniela E. Oprea-Lager[1]

[1]Department of Radiology and Nuclear Medicine, Amsterdam University Medical Centers, Vrije Universiteit Amsterdam, Amsterdam, The Netherlands; [2]Department of Urology, Amsterdam University Medical Centers, Vrije Universiteit Amsterdam, Amsterdam, The Netherlands; [3]Department of Radiology and Nuclear Medicine, Noordwest Ziekenhuisgroep, Alkmaar, The Netherlands; [4]Department of Nuclear Medicine, Zaans Medisch Centrum, Zaandam, The Netherlands; [5]Department of Radiology and Nuclear Medicine, Meander Medisch Centrum, Amersfoort, The Netherlands; and [6]Department of Epidemiology and Biostatistics, Amsterdam University Medical Centers, Amsterdam, The Netherlands

Biochemically recurrent prostate cancer (BCR) is the main indication to perform prostate-specific membrane antigen PET/CT. However, localizing BCR with prostate-specific membrane antigen PET/CT remains challenging in patients with low prostate-specific antigen (PSA) values. Here, we studied the impact of advanced PET image reconstruction methods on BCR localization and interobserver agreement with ^{18}F-DCFPyL PET/CT scans in patients with BCR and low PSA values. **Methods:** Twenty-four patients with BCR and a PSA level of less than 2.0 ng/mL were included. PET images were reconstructed with 4-mm voxels and 2-mm voxels, both with and without point-spread function. All scans were interpreted by 4 nuclear medicine physicians. Additionally, PET examinations of 5 patients with primary prostate cancer and confirmed absence of lymph node metastases (after lymph node dissection) were included, to assess the risk of introducing false-positive findings when using advanced reconstruction. Calculation of BCR localization rates (scan positivity) was based on consensus among our readers ($\geq$3 readers regarding a scan positive for BCR), as well as the individual scan interpretations of the readers. **Results:** In the consensus analysis, BCR localization rates were not higher using advanced reconstruction (62.5%–66.7%) than using 4-mm reconstruction (62.5%). On the basis of individual readings, however, more scans were positive using 2-mm reconstruction (74.0%; 95% confidence interval [CI], 65.0%–82.9%) ($P = 0.027$) and 2-mm reconstruction with point-spread function (75.0%; 95% CI, 66.2%–83.8%) ($P = 0.014$) than 4-mm reconstruction (65.6%; 95% CI, 56.0%–75.3%). A higher number of lesions was detected on the 2-mm scans (median, 2 lesions; interquartile range, 1–3) than the 4-mm scans (median, 1; interquartile range, 0–3; $P = 0.008$). The advanced reconstruction methods did not increase interobserver agreement (80.6%–84.7%), compared with the 4-mm scans (75.7%, $P = 0.08$–0.25). In the patients with primary prostate cancer, an equal number of false-positive lesions was observed among the different reconstruction methods (overall, $n = 13$). **Conclusion:** Applying advanced image reconstruction for ^{18}F-DCFPyL PET/CT scans did not increase BCR localization in patients with BCR and low PSA values (reader consensus). Yet, the increased number of positive individual readings may imply that further development of image reconstruction methods holds potential to improve BCR localization. No improved interobserver agreement was observed with advanced reconstruction compared with standard 4-mm reconstruction.

Key Words: prostate cancer; ^{18}F-DCFPyL; image reconstruction; PSMA

Prostate cancer (PCa) is the most common cancer in men in the Western world (*1,2*). Since the introduction of tracers that bind the prostate-specific membrane antigen (PSMA), PET/CT has been increasingly used for PCa diagnostics. PSMA is a class II transmembrane glycoprotein that provides a valuable target for radiolabeled imaging, as it is significantly overexpressed in malignant prostate cells (*3*).

Currently, the main indication for PSMA PET imaging is the localization of biochemically recurrent PCa (BCR) after initial therapy with curative intent (*4*). BCR is defined by 2 consecutive prostate-specific antigen (PSA) values of at least 0.2 ng/mL after radical prostatectomy, or any PSA value 2.0 ng/mL above the nadir after radiation therapy (*5,6*). Early lesion localization of BCR is desired for directing further treatment, which might include targeted radiotherapy or surgery (*6*). For localization of BCR, ^{68}Ga-labeled PSMA tracers (^{68}Ga-PSMA-HBED-CC) appear promising (*4,7,8*). Alternatively, ^{18}F-labeled PSMA tracers have been developed, most notably ^{18}F-DCFPyL (2-(3-{1-carboxy-5-[(6-^{18}F-fluoro-pyridine-3-carbonyl)-amino]-pentyl}-ureido)-pentanedioic acid) (*9,10*) and ^{18}F-PSMA-1007 (*11*). Because of a shorter positron range and higher positron yield, ^{18}F provides a higher PET image resolution than ^{68}Ga and thus may improve detection of small metastases (*4*). Indeed, ^{18}F-DCFPyL PET/CT revealed enhanced localization of BCR compared with ^{68}Ga-PSMA PET/CT in first clinical analyses (*12,13*).

PET acquisitions can be reconstructed using various methods. Typically, images are created with a voxel size of around 4 mm

(14–16). However, modern PET techniques and reconstruction algorithms allow images with a higher resolution, resulting in voxels of 2 mm. Additionally, reconstruction algorithms may include point-spread function (PSF), which can increase the spatial resolution and signal-to-noise ratio (17,18). For PSMA PET, these advanced image reconstruction methods may influence the detection of small lesions suspected of being BCR, especially when a ^{18}F-labeled tracer is used. This may be especially relevant for patients with BCR and a low PSA value (<2.0 ng/mL), in whom lesion detection with PSMA PET could still be improved (localization rate, 11%–80%) (7,12,15). Hence, the aim of this study was to evaluate if advanced PET image reconstruction for ^{18}F-DCFPyL PET/CT affects lesion detection in patients with BCR and low PSA values.

Limited information is available about interobserver agreement on PSMA PET interpretation, and such agreement is a prerequisite for the acceptance of any imaging technique. Therefore, this study additionally assessed interobserver agreement on ^{18}F-DCFPyL PET/CT interpretation and studied the effect of different image reconstruction methods on agreement. For this assessment, we included the proposed standardized interpretation systems PSMA Reporting and Data System (PSMA-RADS) (19) and Prostate Cancer Molecular Imaging Standardized Evaluation (PROMISE) (20).

MATERIALS AND METHODS

Design

This was a comparative analysis of different image reconstruction methods (4-mm, 2-mm, and PSF) for ^{18}F-DCFPyL PET/CT scans in patients with BCR, using single-center data interpreted by 4 nuclear physicians from different centers.

The study was approved by the institutional review board of the Amsterdam University Medical Centers (review 2018.453), and the need for written informed consent was waived.

Patient Population

Twenty-four consecutive patients were retrospectively included from a single center (Amsterdam University Medical Centers, Vrije Universiteit Amsterdam). Inclusion criteria were newly detected BCR after radical prostatectomy, a current PSA value of less than 2.0 ng/mL,

and the availability of a ^{18}F-DCFPyL PET/CT scan. Patients were excluded if they received androgen deprivation therapy or other oncologic treatment at the time of the ^{18}F-DCFPyL PET/CT scan.

Histologic verification of PSMA PET findings for BCR (e.g., through histologic biopsy) is often difficult and therefore scarcely performed. Advanced image reconstruction may offer early detection of PCa lesions but may also result in false-positive findings. To assess the added risk of false-positive findings when using advanced reconstruction, we additionally included 5 primary-PCa patients. Inclusion criteria for these patients were histologically confirmed PCa treated with radical prostatectomy in combination with extended lymph node dissection, the availability of a preoperative ^{18}F-DCFPyL PET/CT scan, and confirmed absence of lymph node metastases on histopathologic examination. Given the absence of nodal metastases, any suggestive lymph node detected with ^{18}F-DCFPyL PET/CT (any reconstruction) was considered a false-positive result.

Imaging Protocol and Image-Reconstruction Methods

Routine clinical PET examinations were obtained from the Amsterdam University Medical Centers and included a low-dose CT scan (30 mAs, 120 kV). ^{18}F-DCFPyL was synthesized under good-manufacturing-practice conditions at our own department (Radionuclide Center, Amsterdam University Medical Centers) using the precursor of ABX (ABX GmbH). The median administered dose of ^{18}F-DCFPyL was 314.4 MBq (range, 257.7–328.6 MBq), with a median uptake time of 120 min (range, 99–142 min). No diuretics were administered before the scan. Imaging was performed with a hybrid Philips Ingenuity TF scanner (Philips Healthcare) (crystal size, $4 \times 4 \times 22$ mm; 18-cm axial field of view; system sensitivity, 7.3 cps kBq^{-1}) (21,22). The scan trajectory included mid thighs to skull vertex (4 min per bed position, 50% overlap). Images were corrected for decay, scatter, and random coincidences; photon attenuation was performed using low-dose CT.

The default blob-based ordered-subsets expectation maximization algorithm with time-of-flight reconstruction was used (3 iterations; 33 subsets) (23). For every PET examination (for patients with BCR and patients with primary PCa alike), images with $4 \times 4 \times 4$ mm and $2 \times 2 \times 2$ mm voxels were reconstructed (matrix size, 144×144; slice thickness, 4 mm; matrix size, 288×288; slice thickness, 2 mm). The 4-mm and 2-mm reconstruction methods were subsequently performed including PSF. The reconstruction methods are referred to here as 4 mm, 4 mm+PSF, 2 mm, and 2 mm+PSF. An illustration of images obtained with the 4 reconstruction methods is presented in Figure 1.

Image Interpretation

Scans were interpreted independently by 4 nuclear medicine physicians from different institutes, all with ample experience in ^{18}F-DCFPyL PET scan reading (>200 scans). All scans were anonymized and presented in random order during 5 reading sessions over several months' time. The readers were masked to clinical data, except for the indication for the scan (primary staging or BCR). Specifically, the readers were unaware that the patients scanned for primary staging all had a confirmed negative lymph node status.

The readers assessed whether suspected lesions were present in the prostate bed, lymph nodes, bone, or visceral organs (routine clinical evaluation); they considered a scan positive if at least 1 lesion suggestive of BCR was detected. For all individual lesions, a Likert score was given to assess readers' diagnostic
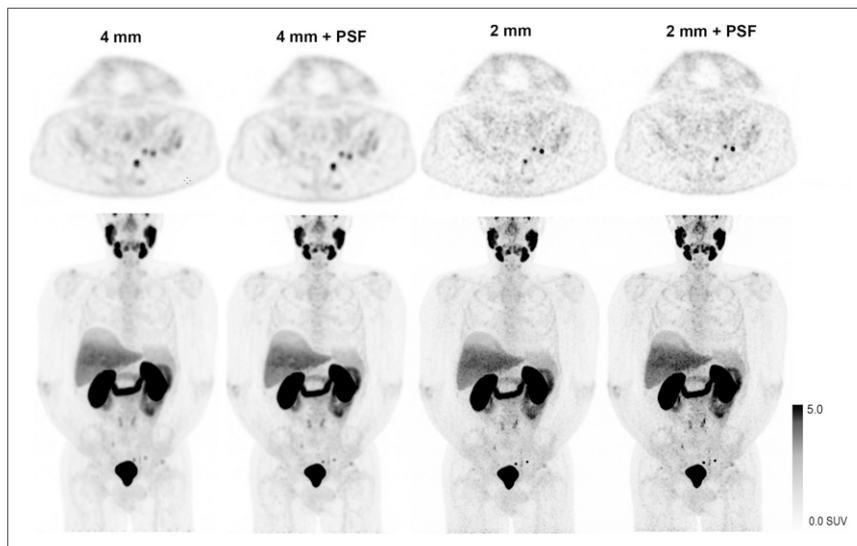
FIGURE 1. Example of 4 image reconstruction methods from 1 patient. Maximum-intensity projections (bottom) and axial images (top) with identical scaling are shown.

TABLE 1
Patient and Scan Characteristics

Characteristic	BCR* (n = 24)		Primary staging† (n = 5)	
	Median	Range	Median	Range
Age (y)	67	61–77	63	55–69
PSA (ng/mL)	0.7	0.4–1.9	8.7	7.2–26.8
Gleason score	7	6–9	7	7–8
Tumor stage	3a	2a–4	3a	—
Injected dose (MBq)	314.3	257.7–328.6	318.8	299.0–325.9
Uptake time (min)	120	99–142	123	117–164

*Inclusion period: November 2017–October 2018.
†Inclusion period: November 2017–February 2018.
Data are based on prostatectomy specimens.

confidence (1 = PCa very unlikely; 2 = PCa unlikely; 3 = unclear/PCa possible; 4 = PCa likely; and 5 = PCa very likely). In the first 12 BCR patients and the 5 primary-PCa patients, the readers were additionally asked to characterize all lesions using the standardized classification systems PSMA-RADS (19) and PROMISE (20). In short, PSMA-RADS identifies 5 categories (PSMA-RADS 1–2, benign; PSMA-RADS 3, equivocal; and PSMA-RADS 4–5, likely PCa) based on PSMA uptake and a list of predefined findings on conventional imaging (19). In the PROMISE system, lesions are given an expression score (i.e., tracer uptake in the lesion is equal to or higher than that in the blood pool, liver, or salivary glands). With these scores, flowcharts can be consulted to classify a lesion as positive, equivocal, or negative (20).

Statistical Analysis

Numeric variables were summarized with their means, medians, and ranges; categoric variables were summarized with proportions (percentages), including 95% confidence intervals (CIs). The 4 interpretations of the readers were gathered per scan. Final scan positivity was based on the existence of a consensus among the readers, with consensus being defined as at least 3 readers detecting 1 or more lesions suggestive of BCR. The scan positivity rates of advanced reconstruction were compared with 4-mm reconstruction (clinical standard). Additionally, the scan positivity rate and the average number of detected lesions were calculated per reconstruction method, on the basis of all individual readings. Differences between reconstruction methods (individual readings) were

compared in a repeated-measures analysis using generalized linear mixed models (binary logistic model [scan positivity rate] and Poisson log-linear model [number of lesions], with the observers as within-subject variable and the reconstruction methods as fixed effect) (supplemental materials, available at http://jnm.snmjournals.org). For the primary staging scans, only the individual readings were assessed, as the question in that case was how frequently false-positive findings are reported by individual readers.

To assess interobserver variability, the proportion of agreement was calculated (24). Differences in agreement per reconstruction method were analyzed with the generalized linear mixed models as described above. The significance level was set at a P value of 0.05. Statistical modeling was performed with STATA, version 14.

RESULTS

BCR Localization Rates

The BCR patients had a median PSA value of 0.7 ng/mL (Table 1). On the basis of the consensus scores, no substantial differences were observed in the scan positivity rate of advanced reconstruction methods compared with the 4-mm scans (Table 2). However, on the basis of individual readings, more scans were positive using the 2-mm (74.0%; CI, 65.0%–82.9%) (P = 0.027) and 2-mm+PSF reconstruction methods (75.0%, CI 66.2%–83.8%) (P = 0.014) than using the 4-mm reconstruction (65.6%; CI, 56.0%–75.3%). A higher number of lesions was detected on the 2-mm scans (median, 2 lesions; interquartile range, 1–3) than on the 4-mm scans (median, 1; interquartile range, 0–3; P = 0.008) (Table 2).

Most scans were positive because of suggestive lymph nodes (38.8% of all scans) or recurrences in the prostate bed (27.6%) (Table 3). The extra positive scan interpretations (individual readings) with the 2-mm and 2-mm+PSF reconstruction methods mostly included additional identification of lesions in the prostate bed (7/13 scan evaluations that were positive only with the 2-mm or 2-mm+PSF reconstruction). Figure 2 provides illustrations.

Interobserver Agreement of BCR Scans

Advanced scan reconstruction did not significantly enhance interobserver agreement in this study (proportional agreement of 82.6%–84.7% with advanced reconstruction vs. 78.5% with 4-mm reconstruction) (Table 4). The positive agreement (83.6%–89.8%) was higher than the negative agreement (66.7%–74.7%) in all reconstruction methods (Table 4).

TABLE 2
Localization of BCR

Reconstruction method	Localization rate			Detected lesions (n)				
	Consensus analysis (≥3 readers)	95% CI	Individual readings	95% CI	Mean	Median	IQR
4 mm	15/24 (62.5%)	41.6%–83.4%	63/96 (65.6%)	56.0%–75.3%	2.2	1	0–3
4 mm+PSF	15/24 (62.5%)	41.6%–83.4%	63/96 (65.6%)	56.0%–75.3%	2.1	1	0–3
2 mm	16/24 (66.7%)	46.3%–87.0%	71/96*(74.0%)	65.0%–82.9%	2.8*	2	1–3
2 mm+PSF	16/24 (66.7%)	46.3%–87.0%	72/96*(75.0%)	66.2%–83.8%	2.4	1	0–3

*Significantly different from 4-mm reconstruction.
IQR = interquartile range.
Data are scan positivity rate; number of detected lesions.

TABLE 3
Scan Evaluations Including 1 or More Lesions per Anatomic Location

Location	Scan evaluations	Total lesions
Prostate bed	106 (27.6%)	106 (13.0%)
Lymph nodes	149 (38.8%)	454 (55.8%)
Bone	91 (23.7%)	241 (29.6%)
Viscera	7 (1.8%)	7 (0.9%)
Other/missing	3 (0.8%)	6 (0.7%)
No detected lesions	120 (31.3%)	

Data are total number of lesions detected per anatomic location.

Primary Staging

In total, 13 suggestive observations outside the prostate were described in any of the individual scan interpretations. In 1 patient, a single suspected left femur lesion was described by 3 readers in all 4 image reconstruction methods (12 observations). The single other detected lesion involved a suggestive lymph node, observed only by 1 reader, in a 4-mm+PSF scan. For both patients, the PSA levels after radical prostatectomy remained undetectable, suggesting that the observed lesions comprised false-positive results (current PSA follow-up, 14 mo and 10 mo). All other scans were negative for metastatic PCa.

Lesion Characterization Using Standardized Classification Systems

An overview of the scores of individual lesions is given in Table 5. The PSMA-RADS score was equal to the Likert score in 86.8% of all lesions (452/521). The PROMISE conclusion was equal to the Likert score in 91.4% of lesions (476/521) when the PROMISE score of equivocal and the Likert score of 3 were interpreted as positive (the PROMISE protocol hardly ever appoints equivocal scores). Different scores were observed primarily for lesions with a Likert score of 1–3. Of all lesions with a Likert score of 1–2 (PCa unlikely), 26.3% (10/38 lesions) were scored as positive using PROMISE and 57.9% (22/38) were scored as equivocal using PSMA-RADS. Of all lesions with a Likert score of 3 (PCa possible), 67.6% (50/74 lesions) had a positive PROMISE outcome and 24.3% (18/74) had a positive PSMA-RADS score.

If scan positivity were based only on PSMA-RADS (i.e., score 4–5 is positive) instead of on the readers' routine clinical evaluation, 2 individual scan interpretations would be different (1.0% of the first 12 BCR scans; both evaluations would become positive). If scan positivity were based on the PROMISE protocol, 7 scan interpretations would be different (3.6%; 2 scans would be positive and 5 negative).

In 1 primary staging scan, a false-positive bone lesion was observed. The lesion was mostly rated as equivocal on the Likert scale (8/12 ratings were a 3) as well as on PSMA-RADS (7/12 ratings were a 3). Yet, using PROMISE, all 12 lesions were rated as positive.

### Interobserver Agreement on Lesion Characterization

All lesions that were described by 2 or more readers were identified. To avoid double-counting of lesions in multiple image reconstruction methods, only the 2-mm scans were analyzed (most available lesions). Thirty-one lesions were identified (16 by 4 readers, 8 by 3 readers, and 7 by 2 readers; total readings, 102). The proportion of overall agreement was 84.9% (CI, 76.4%–91.3%) using the Likert scale; 83.3% (CI, 74.5%–90.1%) with PSMA-RADS; and 93.7% (CI, 87.0%–97.6%) with PROMISE. The proportional agreement for the expression score, used in PROMISE, was 42.9% (CI, 32.9%–53.2%).

DISCUSSION

In this study, different image reconstruction methods for ^{18}F-DCFPyL PET/CT scans were evaluated in terms of lesion detection and interobserver agreement in patients with BCR and low PSA values. On the basis of reader consensus, no higher BCR localization rates were observed when advanced image reconstruction (2 mm) was used than when standard scans (4 mm) were used. The proportional interobserver agreement was higher with advanced reconstruction (82.6%–84.7%) than with the 4-mm scan (78.5%), but the difference was not statistically significant (Table 4).

In clinical practice, PSMA PET scans are most often evaluated by a single reader. When looking at the individual scan interpretations, the 2-mm or 2-mm+PSF reconstruction resulted in 8%–9% more positive scan evaluations (absolute percentage), with an increased number of detected lesions (Table 2). Taken altogether, our data do not support a strong recommendation for any advanced reconstruction method over the standard 4-mm reconstruction. Yet, the increased number of positive individual readings may imply that further development of image reconstruction methods holds potential to improve BCR localization. It should be noted that for every individual patient, 4 different scans were created (4 reconstruction methods). The number of individual patients we could include was
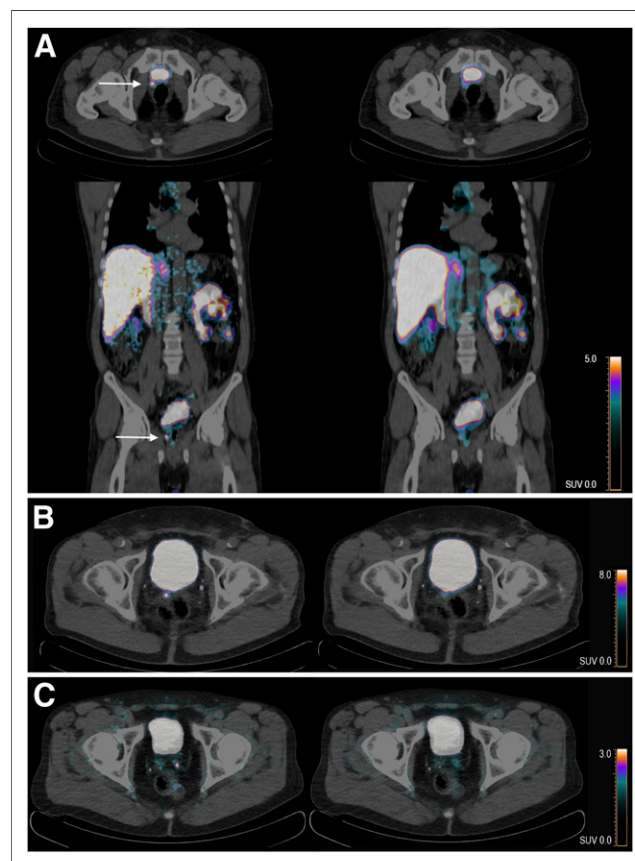
FIGURE 2. Additional detection of local recurrence (arrows) on 2-mm scan (left) compared with 4-mm scan (right). Panels A, B, and C each illustrates a different patient.

TABLE 4
Interobserver Agreement Scores

Reconstruction method	Complete agreement	Proportional agreement		
		Overall	Positive agreement	Negative agreement
4 mm	14/24 (58.3%)	78.5% (69.8%–85.7%)	83.6% (73.2%–91.1%)	68.7% (51.9%–82.5%)
4 mm+PSF	16/24 (66.7%)	82.6% (74.4%–89.1%)	86.8% (77.0%–93.5%)	74.7% (58.4%–87.2%)
2 mm	16/24 (66.7%)	82.6% (74.4%–89.1%)	88.3% (79.4%–94.3%)	66.7% (47.1%–82.8%)
2 mm+PSF	18/24 (75.0%)	84.7% (76.8%–90.8%)	89.8% (81.4%–95.3%)	69.4% (49.5%–85.2%)

Data are for equal interpretation (either positive or negative) of scan by all 4 readers. Data in parentheses are 95% CIs.

thus limited, as was the statistical power to detect differences in lesion detection. As such, our results may rather be considered as hypothesis-generating, pointing toward increased-resolution PSMA PET scans (2 mm) to enhance diagnostics.

For the individual patient, increased BCR localization may be clinically relevant, as PSMA PET outcomes influence therapeutic decisions on salvage local interventions, metastasis-directed therapy, or the initiation of systemic treatment (6,25,26). However, improved detection of lesions alone does not necessarily improve patient outcomes. There is an evident need to assess the effect of PSMA PET–based treatment on clinical outcomes (e.g., time to start androgen deprivation therapy, progression-free survival, and overall survival) (6,27). We believe these prospective evaluations may incorporate the use of advanced reconstruction methods.

The positivity rate with 4-mm scans in this study (63% in the consensus analysis; 66% based on individual interpretations) is in line with previous results using ^{68}Ga-PSMA PET/CT for patients with similar PSA values (7,15). A prior study on ^{18}F-DCFPyL PET/CT by Dietlein et al. (12) used an advanced reconstruction method as well (2- to 3-mm voxels, including PSF). It reported a scan positivity rate comparable to that in our study with the 2-mm+PSF scans for patients with similar PSA values (67% in consensus analysis; 75% based on individual readings).

An important limitation of many studies on PSMA PET for BCR is the lack of histopathologic confirmation of PSMA PET results (7,12,15). PSMA PET–detected lesions are often smaller than 1 cm, making biopsy procedures difficult and burdensome for patients. Without knowing the exact number of PCa metastases, the true diagnostic accuracy of PMSA PET cannot be assessed, however (neither for regular scans nor for advanced image

reconstruction). To estimate the added risk of false-positive findings when using advanced image reconstruction, we included patients with confirmed absence of lymph node metastases. No increase in false-positive findings was observed in these patients when advanced reconstruction was applied. Although these outcomes are encouraging, these result are based on only a small number of primary-PCa patients. In our BCR patients, we did not perform true histologic verification of lesions additionally detected with advanced image reconstruction.

If histologic confirmation is not possible, clinical follow-up can provide another means to confirm the nature of detected lesions. Although the follow-up period of this study was limited (often <1 y), some clinical observations are worth mentioning. In 1 patient, many (>5) bone metastases were suspected by all readers in all image reconstruction methods. These lesions were again reported on bone scintigraphy 2 mo later, substantiating their metastatic nature. In 2 other patients, the detected lesions (a local recurrence and a suspected bone lesion) were later confirmed on follow-up ^{18}F-DCFPyL PET/CT scans. Further, 1 patient received radiation therapy targeted on a local recurrence in the prostate bed, which resulted in a substantial PSA decrease. This lesion was described by all readers on the 2-mm scans but was missed by 1 reader on a 4-mm scan. Another patient received routine, masked radiotherapy on the prostate bed (the clinical PET interpretation was negative), and an immediate PSA decrease followed. In our study, a local recurrence was suspected in this patient on a 2-mm scan. Clearly, these clinical observations come with many limitations of their own. However, together with the results for the primary staging scans, the observations may substantiate the validity of our findings in the absence of a golden standard.

TABLE 5
Lesion Characterization Using Different Interpretation Protocols

Likert score (n)	PSMA-RADS			PROMISE		
	1–2	3A–3D	4–5	Negative	Equivocal	Positive
1–2: PCa unlikely (n = 38*)	15	22	0	25	1	11
3: unclear/PCa possible (n = 74†)	2	53	18	22	2	50
4–5: PCa likely (n = 409)	1	24	384	10	0	399

*1 missing PSMA-RADS and PROMISE score.
†1 missing PSMA-RADS score.
Total numbers are presented (Likert and PSMA-RADS categories 1–2 and 4–5 are taken together; i.e., PCa unlikely, PCa likely).

In our patients with BCR and low PSA values, we anticipated mainly small-lesion detection, which is thought to be enhanced by PSF (17,21). No improved diagnostic results were observed for PSF, however. In this first evaluation of PSF for BCR localization, we used only the standard PSF reconstruction settings. Potentially, further development may improve diagnostic outcomes, for PSF has been shown to benefit from thorough optimization of all reconstruction parameters to balance contrast recovery versus noise induction (18).

The interobserver agreement in this study appeared generally satisfactory, although the relatively low negative agreement scores (67%–75%) might imply that dual reading of negative scans is still advisable (16). The use of standardized reading protocols had a limited effect on scan interpretation (positive or negative), as may be expected when the observer agreement is already satisfactory. On a lesion level, use of the PROMISE protocol resulted in many positive (i.e., malignant) classifications (Table 4). The interobserver agreement for the proposed expression score was low (43%), however, causing concern about the many positive classifications. Our readers reported feeling uncomfortable with some positive classifications using PROMISE, as was illustrated by the false-positive findings in the primary PCa patients: all these lesions were rated as equivocal on routine clinical interpretation but positive using PROMISE. Recently, Yin et al. presented follow-up data on equivocal lesions (PSMA-RADS 3). In line with our experience, they conclude that clinically dubious lesions are truly indeterminate and certainly not always cancer (28).

Our study has limitations regarding the analysis of interobserver agreement, and overall, we were unable to demonstrate a clear benefit of the PSMA-RADS or PROMISE protocol. The lack of histologic characterization of individual lesions hampers accurate comparison of the classification systems. Lastly, our readers reported primarily the findings they found clinically relevant, that is, potentially malignant. It is possible that dubious lesions were described by some readers (who interpreted the lesions as malignant) but omitted by others (who interpreted the lesions as benign). Such lesions would consequently not be included in the interobserver agreement analysis, inflating our results on agreement on a lesion basis.

CONCLUSION

In this study, we evaluated the impact of advanced image reconstruction methods for ^{18}F-DCFPyL PET/CT on lesion detection and interobserver agreement, in patients with BCR and low PSA values. On the basis of reader consensus, the advanced image reconstruction methods did not result in higher BCR localization rates. Yet, an increased number of positive individual scan interpretations was observed when 2-mm scans were used, implying that further development of image reconstruction methods may hold potential to improve BCR localization. Given our limited sample size, future research is warranted to confirm these results. No improved interobserver agreement was observed with advanced reconstruction compared with standard 4-mm reconstruction.

DISCLOSURE

KEY POINTS

QUESTION: Does advanced PET image reconstruction for ^{18}F-DCFPyL PET/CT affect lesion detection in patients with biochemically recurrent PCa and low PSA values?

PERTINENT FINDINGS: On the basis of a reader consensus analysis, application of advanced image reconstruction for ^{18}F-DCFPyL PET/CT did not increase localization of recurrent PCa. However, on the basis of individual readings (i.e., clinical practice), an increased number of positive scans was observed and more lesions were detected when advanced imaging reconstruction was used.

IMPLICATIONS FOR PATIENT CARE: The increased number of positive, individual scan readings implies that further development of image reconstruction holds potential to improve localization of PCa or recurrent PCa.

REFERENCES

1. Ferlay J, Soerjomataram I, Dikshit R, et al. Cancer incidence and mortality worldwide: sources, methods and major patterns in GLOBOCAN 2012. *Int J Cancer.* 2015;136:E359–E386.
2. Siegel RL, Miller KD, Jemal A. Cancer statistics, 2018. *CA Cancer J Clin.* 2018;68:7–30.
3. Perner S, Hofer MD, Kim R, et al. Prostate-specific membrane antigen expression as a predictor of prostate cancer progression. *Hum Pathol.* 2007;38:696–701.
4. Rowe SP, Gorin MA, Allaf ME, et al. PET imaging of prostate-specific membrane antigen in prostate cancer: current state of the art and future challenges. *Prostate Cancer Prostatic Dis.* 2016;19:223–230.
5. Amling CL, Bergstralh EJ, Blute ML, Slezak JM, Zincke H. Defining prostate specific antigen progression after radical prostatectomy: what is the most appropriate cut point? *J Urol.* 2001;165:1146–1151.
6. Cornford P, Bellmunt J, Bolla M, et al. EAU-ESTRO-SIOG guidelines on prostate cancer. Part II: treatment of relapsing, metastatic, and castration-resistant prostate cancer. *Eur Urol.* 2017;71:630–642.
7. Perera M, Papa N, Christidis D, et al. Sensitivity, specificity, and predictors of positive ^{68}Ga-prostate-specific membrane antigen positron emission tomography in advanced prostate cancer: a systematic review and meta-analysis. *Eur Urol.* 2016;70:926–937.
8. Afshar-Oromieh A, Zechmann CM, Malcher A, et al. Comparison of PET imaging with a ^{68}Ga-labelled PSMA ligand and ^{18}F-choline-based PET/CT for the diagnosis of recurrent prostate cancer. *Eur J Nucl Med Mol Imaging.* 2014;41:11–20.
9. Chen Y, Pullambhatla M, Foss CA, et al. 2-(3-{1-carboxy-5-[(6-[^{18}F]fluoro-pyridine-3-carbonyl)-amino]-pentyl}-ureido)-pentanedioic acid, [^{18}F]DCFPyL, a PSMA-based PET imaging agent for prostate cancer. *Clin Cancer Res.* 2011;17:7645–7653.
10. Szabo Z, Mena E, Rowe SP, et al. Initial evaluation of [^{18}F]DCFPyL for prostate-specific membrane antigen (PSMA)-targeted PET imaging of prostate cancer. *Mol Imaging Biol.* 2015;17:565–574.
11. Giesel FL, Hadaschik B, Cardinale J, et al. F-18 labelled PSMA-1007: biodistribution, radiation dosimetry and histopathological validation of tumor lesions in prostate cancer patients. *Eur J Nucl Med Mol Imaging.* 2017;44:678–688.
12. Dietlein F, Kobe C, Neubauer S, et al. PSA-stratified performance of ^{18}F- and ^{68}Ga-PSMA PET in patients with biochemical recurrence of prostate cancer. *J Nucl Med.* 2017;58:947–952.
13. Wondergem M, Jansen BHE, van der Zant FM, et al. Early lesion detection with ^{18}F-DCFPyL PET/CT in 248 patients with biochemically recurrent prostate cancer. *Eur J Nucl Med Mol Imaging.* 2019;46:1911–1918.
14. Boellaard R, Delgado-Bolton R, Oyen WJ, et al. FDG PET/CT: EANM procedure guidelines for tumour imaging: version 2.0. *Eur J Nucl Med Mol Imaging.* 2015;42:328–354.
15. Afshar-Oromieh A, Holland-Letz T, Giesel FL, et al. Diagnostic performance of ^{68}Ga-PSMA-11 (HBED-CC) PET/CT in patients with recurrent prostate cancer: evaluation in 1007 patients. *Eur J Nucl Med Mol Imaging.* 2017;44:1258–1268.
16. Burggraaff CN, Cornelisse AC, Hoekstra OS, et al. Interobserver agreement of interim and end-of-treatment ^{18}F-FDG PET/CT in diffuse large B-cell lymphoma: impact on clinical practice and trials. *J Nucl Med.* 2018;59:1831–1836.

17. Andersen FL, Klausen TL, Loft A, Beyer T, Holm S. Clinical evaluation of PET image reconstruction using a spatial resolution model. *Eur J Radiol.* 2013;82: 862–869.

18. Akamatsu G, Ishikawa K, Mitsumoto K, et al. Improvement in PET/CT image quality with a combination of point-spread function and time-of-flight in relation to reconstruction parameters. *J Nucl Med.* 2012;53:1716–1722.

19. Rowe SP, Pienta KJ, Pomper MG, Gorin MA. Proposal for a structured reporting system for prostate-specific membrane antigen-targeted PET imaging: PSMA-RADS version 1.0. *J Nucl Med.* 2018;59:479–485.

20. Eiber M, Herrmann K, Calais J, et al. Prostate Cancer Molecular Imaging Standardized Evaluation (PROMISE): proposed miTNM classification for the interpretation of PSMA-ligand PET/CT. *J Nucl Med.* 2018;59:469–478.

21. van der Vos CS, Koopman D, Rijnsdorp S, et al. Quantification, improvement, and harmonization of small lesion detection with state-of-the-art PET. *Eur J Nucl Med Mol Imaging.* 2017;44:4–16.

22. Kolthammer JA, Su KH, Grover A, Narayanan M, Jordan DW, Muzic RF. Performance evaluation of the Ingenuity TF PET/CT scanner with a focus on high count-rate conditions. *Phys Med Biol.* 2014;59:3843–3859.

23. Popescu LM, Matej S, Lewitt RM. Iterative image reconstruction using geometrically ordered subsets with list-mode data. In: *IEEE Symposium Conference Record Nuclear Science 2004*. Piscataway, NJ: IEEE; 2004: 3536–3540.

24. de Vet HC, Mokkink LB, Terwee CB, Hoekstra OS, Knol DL. Clinicians are right not to like Cohen's kappa. *BMJ.* 2013;346:f2125.

25. Emmett L, van Leeuwen PJ, Nandurkar R, et al. Treatment outcomes from ^{68}Ga-PSMA PET/CT-informed salvage radiation treatment in men with rising PSA after radical prostatectomy: prognostic value of a negative PSMA PET. *J Nucl Med.* 2017;58:1972–1976.

26. Grubmüller B, Baltzer P, D'Andrea D, et al. ^{68}Ga-PSMA 11 ligand PET imaging in patients with biochemical recurrence after radical prostatectomy: diagnostic performance and impact on therapeutic decision-making. *Eur J Nucl Med Mol Imaging.* 2018;45:235–242.

27. Lecouvet FE, Oprea-Lager DE, Liu Y, et al. Use of modern imaging methods to facilitate trials of metastasis-directed therapy for oligometastatic disease in prostate cancer: a consensus recommendation from the EORTC Imaging Group. *Lancet Oncol.* 2018;19:e534–e545.

28. Yin Y, Werner RA, Higuchi T, et al. Follow-up of lesions with equivocal radiotracer uptake on PSMA-targeted PET in patients with prostate cancer: predictive values of the PSMA-RADS-3A and PSMA-RADS-3B categories. *J Nucl Med.* 2019;60: 511–516.